

Available online at www.sciencedirect.com**ScienceDirect**

Energy Procedia 82 (2015) 45 – 50

Energy

Procedia

ATI 2015 - 70th Conference of the ATI Engineering Association

Large-Eddy Simulation of Cycle-Resolved Knock in a Turbocharged SI Engine

Alessandro d'Adamo^a, Sebastiano Breda^a, Giuseppe Cantore^{a*}^a*Department of Engineering "Enzo Ferrari", University of Modena and Reggio Emilia, Via Vivarelli 10, 41125 Modena, Italy*

Abstract

The paper presents a numerical study of cycle-to-cycle variability in a turbocharged GDI engine. The Large-Eddy Simulation technique is adopted in this study in conjunction with the recent ISSIM-LES model for spark-ignition, allowing a dedicated treatment of both the flame kernel formation and flame development phases.

Numerical results are compared with an extended dataset of experimental test-bed acquisitions, where the engine is operated at knock-limited spark advance.

The agreement of both ensemble averaged combustion pressure history and of its standard deviation confirm the validity of the adopted numerical framework able to correctly quantify the degree of CCV measured by the experiments. Knock tendency is evaluated by means of an in-house developed knock model, based on a tabulation technique for AI delays of the same RON98 gasoline as the one used in experiments. The results confirm the knock-free condition of the experimental KLSA, for which the cycle-resolved knock signature is extremely weak just for the cycles in the highest band of the CCV-affected combustion. The visualization of the pressure wave allows to identify the exhaust side as the most knock-prone region.

Finally, spark-advance is increased by 3 CA with respect to the experimental edge-of knock limit, in order to simulate an experimentally prevented operating condition. Local pressure measurements mimicking flush-mounted transducers confirm the severe knock damage related to this condition. The predictive capability of the combustion CCV and of the adopted knock model confirm the heavy and recurrent cycle-resolved knock damage.

© 2015 The Authors. Published by Elsevier Ltd. This is an open access article under the CC BY-NC-ND license

(<http://creativecommons.org/licenses/by-nc-nd/4.0/>).

Peer-review under responsibility of the Scientific Committee of ATI 2015

Keywords: LES; knock; combustion; CCV

1. Introduction

The recent legislation is moving the engine design focus towards reduced tailpipe emissions. In order to meet these requirements without performance loss, higher and higher power density is requested to modern units. In the field of Spark-Ignition (SI) engines, this is achieved by increasing the volumetric

* Corresponding author. Tel.: +39-0592056115; fax: +39-0592056126.

E-mail address: alessandro.dadamo@unimore.it

compression ratio and/or the boost pressure level. Both these strategies are limited by the occurrence of abnormal combustion events, often referred to as autoignition or 'engine knock'. Since the engine operating condition is required to be as close as possible to the onset of such unwanted phenomena, the need of accurate and robust numerical tools arise in order to accurately identify the 'edge of knock' condition. In this study a modern GDI turbocharged engine for which experimental acquisitions are available is analyzed at the edge of knock, and an in-house developed numerical tool for knock prediction is evaluated. The use of the Large-Eddy Simulation (LES) approach allows to simulate the cyclic fluctuation of combustion, the consequence being that knock as well is simulated as a cycle-dependent phenomenon. This is referred to as 'knock signature' and corresponds to the experimental practice, where a dataset of cycles is evaluated before judging the operating point as knock affected or knock-safe. In the first part of the paper the numerical framework adopted in this study is presented; the agreement between the combustion simulation results and the experimental data is shown. The negligible intensity or absence of heat release by autoignition for all the simulated cycles is in agreement with the experimental outcome and it is a preliminary confirmation of the knock model validity. In the second part the operating point is numerically moved into an experimentally prevented condition, due to engine knock: the knock tool used in the simulation predicts moderate to intense knock for a majority of the simulated cycles, further confirming the physical soundness of the presented model.

Nomenclature

AI	Autoignition
CCV	Cycle-to-Cycle Variability
FSD	Flame Surface Density
KLSA	Knock-Limited Spark Advance
LES	Large-Eddy Simulation
SA	Spark-Advance
SI	Spark-Ignition
TRF	Toluene Reference Fuel

2. Numerical Model

A numerical grid dedicated to Large-Eddy Simulation is created in the environment, comprising both intake and exhaust ports. The resulting number of cells is about 910000 at TDC and 1.5M at BDC, with an average cell size of about 0.5 mm. The complete mesh with intake and exhaust ports and a close-up of the cylinder domain are reported in Fig.1. Subgrid scale turbulence is modelled by the algebraic Smagorinsky model [1], which belongs to the eddy-viscosity closure models and which is based on the hypothesis of a turbulent equilibrium for the subgrid scales. A mean gradient assumption allows to relate subgrid scale dissipation effects to a turbulent viscosity μ_t^{SGS} calculated as $0.202 \cdot \Delta^2 \cdot \Pi_{(S)}^{1/2}$. In the previous equation 0.202 is the Smagorinsky constant, Δ is the average cell size and $\langle S \rangle$ is the filtered strain rate due to the resolved scales.

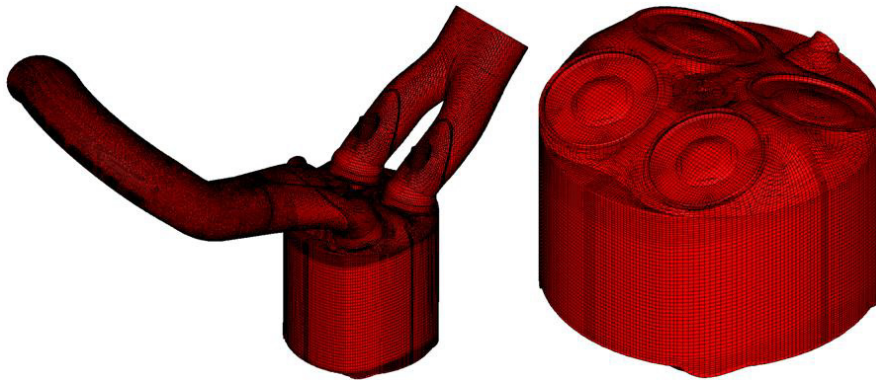


Fig. 1. Computational grid used for LES simulations (a) complete fluid domain; (b) cylinder domain close-up

As for two-phase flows, a Lagrangian treatment is adopted for fuel spray. A pre-atomized population of droplets is imposed at each nozzle exit, while secondary break-up is simulated using the Reitz and Diwakar approach [2]. The Angelberger et al. [3] model is adopted for wall heat transfer, while wall temperatures are derived from a calibrated 1-D model of the engine provided by the engine manufacturer. As for boundary conditions, experimentally derived time-varying pressure and temperature traces are imposed at the domain inlet and outlet. Combustion is modelled by the ECFM-LES combustion model, which is based on the ECFM-family combustion model formalism here adapted for LES [4-5]. The model belongs to the class of coherent flame models where the evolution of the Flame Surface Density (FSD), i.e. the flame surface area per unit volume, is described by a balance equation which takes into account the effects of strain and curvature (both resolved and unresolved) along with the propagation of the flame itself in laminar unburnt gases zone. The adoption of the ISSIM-LES ignition model [6] allows to accurately simulate the flame kernel formation and development by means of the FSD transport equation, thanks to the use of a modified FSD equation, with the presence of dedicated terms for the subgrid treatment of flame surface density. The model implementation in Star-CD is carried out through a joint cooperation with CD-adapco and it constitutes a fundamental improvement for spark-ignition simulation compared to previous studies by the authors where traditional models for ignition were adopted [7]. The use of ISSIM-LES ignition model allows the simulation, instead of modelling, of the early flame kernel growth to a fully developed flame. Therefore the CCV of flame formation is simulated. This model constitutes a remarkable improvement over traditional spark-ignition models based on the deposition of a resolved profile of fully-burnt gases. The in-house developed knock model adopted in this study is based on a look-up table approach of AI delays from detailed chemistry simulation. The model details were published in [7-8] and the fundamentals are resumed here for the sake of completeness. The end-gas knock chemistry is based on the cell-average values of pressure, temperature and equivalence ratio. The fuel model used for the detailed chemistry simulation is based on the Andrae and Head [9] semi-detailed mechanism for Toluene Reference Fuel (TRF) and a blend for a RON98-E0 gasoline is adopted.

3. Combustion Validation at Knock Limited Spark Advance

The set of thirteen LES combustion cycles obtained with the experimental KLSA is compared with the full dataset of 240 experimental cycles from the engine test bed. The in-cylinder pressure traces are reported in Fig.2 for both experiments and LES simulations.

As visible, simulation results fall within the bounds of the most probable experimental cycles, confirming the validity of the modelling framework adopted regarding flame kernel formation and flame propagation. Pressure levels are omitted due to confidentiality imposed by the engine manufacturer.

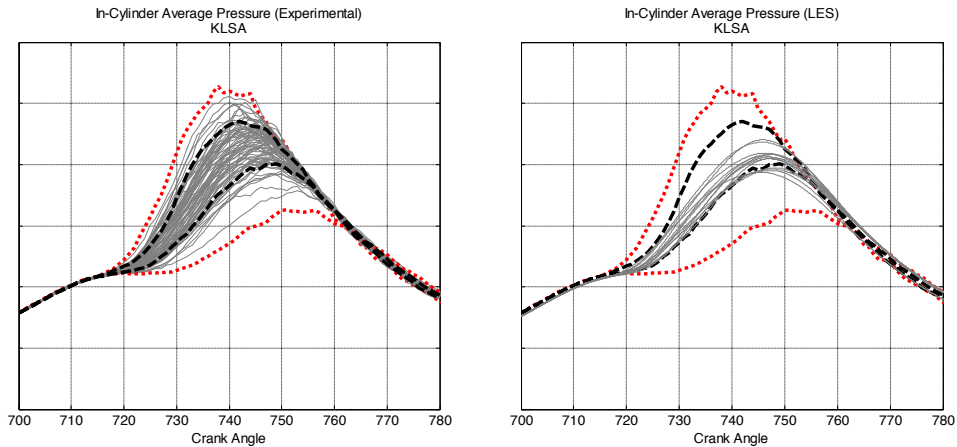


Fig. 2. (a) Experimental cycles (thin grey lines); highest and lowest p_{max} cycles are highlighted (red dashed lines); (b) in-cylinder pressure traces from the 20 LES cycles (thin grey lines); highest and lowest p_{max} cycles from the experiments are highlighted (red dashed lines)

Variations in pressure development are originated by non-repeatability of the combustion process, which is in turn promoted by the cyclic fluctuation of factors such as mixture quality and large-scale flow structures at spark plug. The reduced number of calculated cycles prevents from converged statistics to be carried out; however, the comparison with the experimentally measured peak pressure data reported in Fig. 2 is in excellent agreement in terms of pressure development.

4. Knock Analysis for Knock Limited Spark Advance Condition

In this study the analysis is focused on the confirmation of the knock-limit condition indicated by the experiments. The knocking signature of each cycle can be observed by the in-cylinder heat release rate and by its contribution due to autoignition.

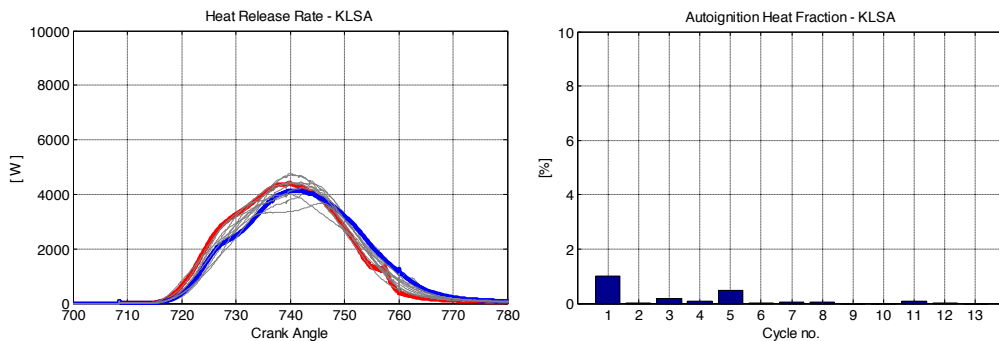


Fig.3. Heat release rate as a function of crank angle at KLSA condition: overall thermal power (a) and contribution due to autoignition (b). Highlighted are the cycle with the highest AI heat fraction (red dashed line) and the lowest one (blue line).

These are reported in Fig. 3 where the cycle with the highest and the lowest portion of heat liberated by autoignition are highlighted (red and blue line, respectively). As visible, weak autoignition is measured

in a fraction of the simulated cycles while most of them are completely free from AI. The largest fraction of heat generated by AI is as low as 1% of the total combustion heat, and it is visible in Fig. 3 (a) as a slight increase of heat release rate at about 755 CA. This confirms the edge of knock operating condition indicated by the experiments and it is a first confirmation of the knock prediction accuracy of the tabulated look-up table approach.

5. Knock Analysis for Increased Spark Advance Condition

The second part of this study deals with the numerical investigation of knock onset for an increased SA. This condition is experimentally prevented in order to avoid destructive knock damage. The set of thirteen combustion cycles at KLSA is repeated for an increase in SA by 3 CA (KLSA+3 condition), in order to evaluate the effect on combustion regularity and knock tendency. In Fig. 4 the thermal power released by combustion and the heat portion released by AI are reported for all the simulated cycles.

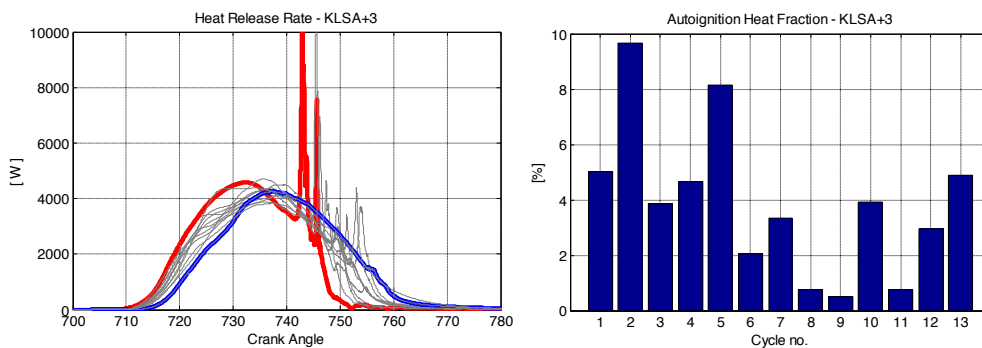


Fig.4. Heat release rate as a function of crank angle at KLSA+3 condition: overall thermal power (left) and contribution due to autoignition (right). Highlighted are the cycle with the highest AI heat fraction (red dashed line) and the lowest one (blue line).

The increase in SA induces higher pressure levels and end-gas thermal loading, thus favouring the conditions for knock onset in a larger fraction of cycles. The fraction of heat released by AI over the entire combustion heat is reported in Fig. 4 (b). Compared to the same measurement relative to KLSA (see Fig. 3 (b)) all the calculated cycles predict a moderate-to-mild fraction of AI heat. Cycle no.2 is the one exhibiting the highest value, with nearly 10% of heat released by AI and an evident knocking trace after 740 CA visible in Fig. 4 (a). On the contrary, the lowest knocking cycle (i.e. Cycle no.9) shows an almost negligible variation in the rate of heat release at 755 CA. This result confirms the virtual engine damaging indicate by the experiments when moving to more advanced SAs than the identified KLSA limit. A final confirmation of the operating point moving into the knocking region when increasing the SA by 3 CA is the visualization of the pressure wave originated by the sudden heat release accompanying knock. This pressure imbalance originated is the main responsible of the damaging mechanisms of the engine components facing the combustion chamber. In Fig. 5 the pressure wave is illustrated. This is defined as the difference between the local pressure and the average in-cylinder pressure \bar{p} at that instant. As visible, it is extremely limited for the heaviest knocking case at KSLA while it is much more intense for the worst cycle at KSLA+3 condition.

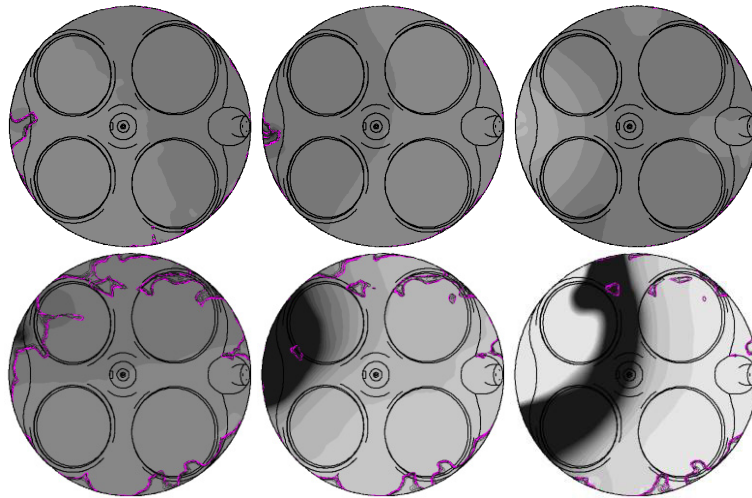


Fig.5. Pressure wave (grey scale) and flame front section (red iso-lines) on a section 2 mm below the flame deck. (a) top row: heaviest knocking cycle at KLSA condition; (b) bottom row: heaviest knocking cycle at KLSA+3 condition. The color scale for pressure wave is limited to ± 5 bar from average pressure. Images are relative to the specific knock onset angle for each case.

6. Conclusion

In this study a currently produced GDI turbocharged unit is analysed at the edge of knock by full-cycle numerical simulations. The Large-Eddy Simulation numerical technique is adopted to simulate cyclic variability. Combustion instability and cycle-dependent knock signature are reproduced by the simulation as well as in the test-bed acquisition. Knock prediction is carried out by an in-house developed tool based on a tabulation of autoignition delay times from a RON98-E0 fuel surrogate model. In the first part of the study the same operating condition is simulated. The peak value of heat fraction liberated by AI as low as 1%, and the absence at all in some cycles, depict a knock-safe condition in agreement with the experimental evidence. In the second part, the operating point is purposely moved into the knocking region by advancing the SA by 3 CA. The same set of combustion cycles shows a cycle-dependent and significant knocking behaviour, with a peak value of heat produced by AI as high as 10%. This result is a second confirmation of the accuracy of the proposed framework for combustion and knock modelling, and it is in line with the experimental engine knock indication for this condition.

References

- [1] Smagorinsky J. *Mon. Wea. Rev.* 91, 99-164.
- [2] Reitz R, Diwakar R. SAE Technical Paper 860469, SAE Trans. 95, 3, 218-227.
- [3] Angelberger C, Poinot T, Delhay B. SAE Paper 972881, doi: 10.4271/972881.
- [4] Vermorel O, Richard S, Colin O, Angelberger C, Benkenida A, Veynante D. *Combustion and Flame* 156 (2009) 1525–1541.
- [5] Richard S, Colin O, Vermorel O, Benkenida A, Angelberger C, Veynante D. *Proc. of the Combustion Institute* 31 (2007) 3059-3066.
- [6] Colin O, Truffin K.. *Proceedings of the Combustion Institute* 33, 3097–3104.
- [7] Fontanesi S, d'Adamo A, Rutland CJ. *International Journal of Engine Research*, published on January 9, 2015 as doi:10.1177/1468087414566253.
- [8] Fontanesi S, Paltrinieri S, d'Adamo A, Cantore G, Rutland CJ. *SAE Int. J. Fuels Lubr.* 6(1):2013, doi:10.4271/2013-01-1082.
- [9] Andrae JCG, Head RA. *HCCI. Combustion and Flame* 156 (2009) 842-851.